



CONCEPTUAL DESIGN OF 180-SEATER PASSENGER AIRCRAFT

SHAHID AMEEN KHAN,

7th semester, Dept. of Aeronautical Engineering,
S. J. C. Institute of Technology,
Chickballapur, India.

shahidameen07@gmail.com

VINAY M R,

7th semester, Dept. of Aeronautical Engineering,
S. J. C. Institute of Technology,
Chickballapur, India.

vinayvini305@gmail.com

KRUTHIKA H V,

7th semester, Dept. of Aeronautical Engineering,
S. J. C. Institute of Technology,
Chickballapur, India.

kruthikahv2001@gmail.com

VIGNESWARAN C M,

Assistant Prof., Dept. of Aeronautical Engineering,
S. J. C. Institute of Technology,
Chickballapur, India.

cmvigneswaranaero@gmail.com

ABSTRACT

This paper presents a study on conceptual design of a 180-seater medium-range passenger aircraft. The main purpose is to understand the importance of aircraft design, the steps involved, and the parameters considered in designing an aircraft with specified mission. The design point is considered by historical data of similar range aircraft- by comparing their weights, power plants used, cruising altitude and speed, service ceiling, and geometrical dimensions of aircraft body. The aircraft will possess a low wing, tricycle landing gear, and a conventional tail arrangement. After the design calculations are complete, the geometry of the aircraft is generated using CATIA V5R20.

Keywords— *Aircraft design, conceptual design process, performance characteristics.*

NOMENCLATURE

A.R. - Aspect ratio
b - Wing span (m)
 c , c_{root} , c_{tip} - chord of the airfoil, chord at root, and chord at the tip, respectively, (m)
 C_L , C_D , C_M - Lift, drag, and moment coefficients, respectively.
M - Mach number of aircraft
 c_t - Thrust specific fuel consumption
(L/D) - Lift to drag ratio
(T/W) - Thrust to weight ratio
m.a.c - Mean aerodynamic chord
c.g - Center of gravity
Re - Reynold's number
 α - Angle of attack, degree
S - Wing area, m^2
E - Endurance, hours
R - Range, kilometers
T- Thrust, kN
I.A.E - International Aero Engines
 V , V_f - Velocity of aircraft, and flare velocity, respectively, m/s
 $r_{takeoff}$ - Radius of turn during takeoff, m
 r_{flare} - Radius of turn during flare, m
 W_{crew} , W_{empty} , W_{gross} , W_{fuel} , W_{PL} - Weight of crew, empty weight of aircraft, gross weight of aircraft, and weight of fuel, payload weight, respectively, kg
 W_m , W_n - Weight of main landing gear wheel, and nose landing gear wheel, respectively, kg
 S_a , S_f , S_g - Approach distance, flare distance, and ground roll distance, respectively, m
 h_{ob} - Height of obstacle, m



I. INTRODUCTION

There are wide range of aircraft classified based on the power – power-driven (airplanes, fighter jets, helicopters, etc.), and non-power driven (gliders, sailplanes, etc.); based on their range – short range aircraft (Phenom 100, Embraer 135, Dornier 328, etc.), short/medium range aircraft (Airbus A320-200, Boeing 737-800, Learjet 60), and long-range aircraft (Airbus A330, Boeing 767-300, Boeing 747-400). There are ultra-long-range private/business aircraft too (Falcon 7X, Gulfstream G550, Boeing Business Jet, etc.); based on the weight or cargo they can carry- small capacity aircraft (Learjet 35, Antonov AN-26, ATR 72F, etc.), medium capacity aircraft- (Boeing 727F, Antonov AN-12, Ilyushin IL-76, etc.), and large capacity aircraft (McDonnell Douglas MD11, Airbus A330, Antonov AN-225, Boeing 747-800F, etc.).

The design process is majorly broken into three phases- conceptual design, preliminary design, and detail design.

A. Conceptual design

Conceptual design is the most important stage in the production and development of an aircraft. The primary components like wings, fuselage, horizontal and vertical stabilizers, and landing gears are defined first. In later design stages, each component is separately designed in detail, considering their geometric aspects, structural and aerodynamic aspects, and performance and stability aspects as well. Conceptual design is a dynamic process- new ideas emerge as the design is investigated in every detail. Each time the latest design or configuration is analyzed and sized, it must be updated to reflect the change in gross weight, and respective changes in fuel weight, wing size, power-plant, fuselage size, etc.

The conceptual design begins with a set of design requirements provided by the customer or the industry. A conceptual sketch is drawn, which includes wing and empennage geometries, the shape of the fuselage, relative location on the engine, cockpit, landing gears and fuel tanks. [4] proposed a principle in which another NN yield input control law was created for an under incited quad rotor UAV which uses the regular limitations of the under incited framework to create virtual control contributions to ensure the UAV tracks a craved direction. Utilizing the versatile back venturing method, every one of the six DOF are effectively followed utilizing just four control inputs while within the sight of un demonstrated flow and limited unsettling influences. Elements and speed vectors were thought to be inaccessible, along these lines a NN eyewitness was intended to recoup the limitless states. At that point, a novel NN virtual control structure which permitted the craved translational speeds to be controlled utilizing the pitch and the move of the UAV. At long last, a NN was used in the figuring of the real control inputs for the UAV dynamic framework. Utilizing Lyapunov systems, it was demonstrated that the estimation blunders of each NN, the spectator, Virtual controller, and the position, introduction, and speed following mistakes were all SGUUB while unwinding the partition Principle.

B. Preliminary design

In the preliminary design phase, aircraft structures, landing gears, and control systems are analyzed. Then testing and inspection is initiated in areas such as aerodynamics, structures, propulsion, and stability and control. A key activity during this phase is 'lofting'. Lofting is the mathematical modeling of outside skin of aircraft with sufficient accuracy to ensure a proper fit between its different parts. The design is carried out by using software packages (like RDS design software from Daniel P. Raymer) that implement analytical methods and empirical relations for sizing of aircraft. The main objective of this phase is to ready the industry for the full-scale development of the aircraft.

C. Detail design

In the detail design phase, the whole aircraft will be broken down into parts, and each part is separately designed and analyzed. Then the specialists determine how the airplane will be fabricated, starting from the smallest and simplest sub-assemblies to the final assembly process. Then the actual structure of the aircraft is tested. The testing effort at this scale intensifies. The design cycle ends with the fabrication of aircraft.

This paper is organized as follows:

- A brief maneuvering tasks performed by the aircraft is depicted in the Section- 'Mission Specification'.
- Historical data of different aircraft is collected, and then major characteristics are computed using analytical and graphical methods.
- Section- 'Weight Estimation' is briefed about the calculation of aircraft weight.



- The selection process for the type of engine is described in Section- 'Power-plant Selection'.
- The design criteria for the wing is interpreted in the Section- 'Wing Geometry'.
- The design of fuselage layout and empennage is presented in Section- 'Fuselage Sizing'.
- The Section- 'Aerodynamic Characteristics' provides the lift estimation, drag estimation, and about various parameters dependent on them.
- The selection of landing gear is presented in the Section- 'Landing Gear Configuration'.
- The aircraft's performance parameters are detailed in the later sections. Finally, the Section- Conclusions, concludes the work presented in this paper.

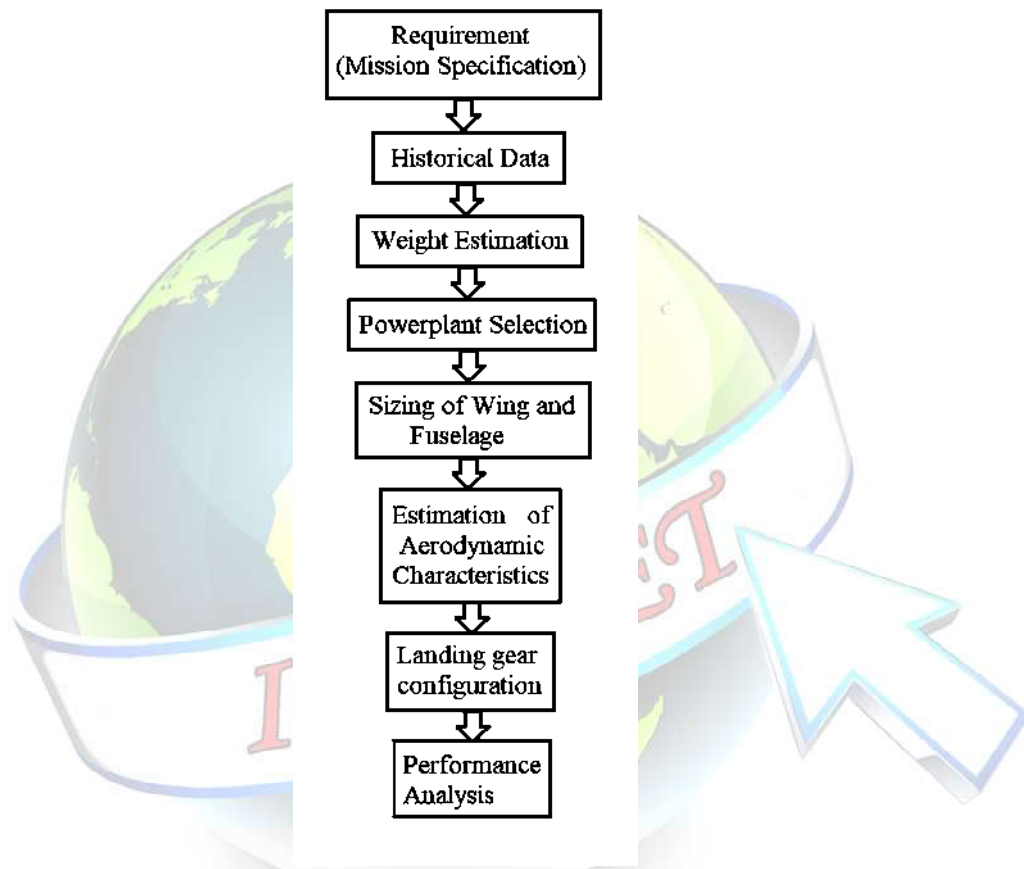


Figure. 1: Design cycle

II. FORMULAE

- Endurance, $E = \frac{\left(\frac{L}{D}\right) * \ln \left[\frac{W_{(gross)}}{W_{(empty)}} \right]}{c_t}$
- Range, $R = \frac{2^{3/2} * C_L^{1/2} * [W_{(gross)}^{1/2} - W_{(empty)}^{1/2}]}{c_t * (\rho * S)^{1/2} * C_D}$
- Payload weight, $W_{PL} = \text{Wt. of passengers} * (\text{Avg. wt. of each passenger} + \text{avg. wt. of each baggage})$
- Mission fuel Weight, $M_{FF} = \frac{W_1}{W_{TO}} * \frac{W_2}{W_1} * \frac{W_3}{W_2} * \frac{W_4}{W_3} * \frac{W_5}{W_4} * \frac{W_6}{W_5} * \frac{W_7}{W_6} * \frac{W_8}{W_7}$
- Fuel weight, $W_{FUEL} = (1 - M_{FF}) * W_{TO(GUESS)}$
- Operational empty weight, $W_{OE(tentative)} = W_{TO(GUESS)} - W_{FUEL} - W_{PL}$



- vii. Take-off weight validation, $W_{TO} = \frac{W_{(payload)}}{1 - \frac{W_{(fuel)}}{W_{(TO)}} - W_{OE(tentative)}}$
- viii. Take-off weight iteration, $W_{TO} = \frac{W_{OE(tentative)}}{A * W_{TO}^c * K_{VS}}$; $A = 1.51$, $c = -0.1$, $K_{VS} = 1$
- ix. Taper ratio, $\lambda = \frac{C_t}{C_r}$
- x. Mean aerodynamic chord, $m.a.c = \frac{\frac{2}{3} * C_r * (1 + \lambda + \lambda^2)}{1 + \lambda}$
- xi. Distance of mean aerodynamic chord from the aircraft centerline = $\frac{b * [1 + (2 * \lambda)]}{6 * (1 + \lambda)}$
- xii. Length of fuselage, $L_{fus} = a * [W_{(gross)}]^b$
- xiii. Length of nose of fuselage, $L_{nose} = 0.03 * L_{fus}$
- xiv. Internal diameter of fuselage, $d_{fus(internal)} = \text{Asile width} + (\text{Seat width} * \text{no. of seats abreast})$
- xv. Fuselage structural thickness, $t_{structural} = (0.02 * \text{internal diameter of cabin}) + 1 \text{ inch}$
- xvi. External diameter of fuselage, $d_{fus(external)} = d_{fus(internal)} + (2 * t_{structural})$
- xvii. Tail length, $L_{tail} = 2.3 * d_{fus(external)}$
- xviii. Lift, $L = \frac{1}{2} * \rho * V^2 * S * C_L$
- xix. Drag, $D = L = \frac{1}{2} * \rho * V^2 * S * C_D$
- xx. Diameter of wheel of landing gear, $d_{wheel} = A * (W_m)^B$
- xxi. Static margin = $\frac{X_{NP} - C.g}{m.a.c}$
- xxii. Aerodynamic center of wing body = $V_{NP} - (V_{HT} * \frac{a_t}{a})$
- xxiii. Ground roll (takeoff), $S_{g(T.O)} = \frac{1.21 * (W_{(gross)})^2}{g * \rho * C_{L(max)} * S * T}$
- xxiv. Radius of turn, $r = \frac{6.96 * (V_{stall})^2}{g}$
- xxv. Distance while airborne to clear obstacle, $S_a = r * \sin \theta_{OB}$
- xxvi. Turn radius during flare, $r_{flare} = \frac{(V_f)^2}{0.2 * g}$
- xxvii. Flare height, $h_f = r_{flare} - (r_{flare} * \cos \theta_f)$
- xxviii. Approach distance, $S_a = \frac{h_{OB} - h_f}{\tan \theta_a}$
- xxix. Flare distance, $S_f = r_{flare} * \sin \theta_f$
- xxx. Ground roll (landing), $S_{g(L)} = (1.15 * N * V_{stall}) + \frac{1.5^2 * (W_{(empty)})^2}{g * \rho * C_{L(max)} * S * [T_{rev} + D + \mu_r * (W_{empty} - L)] + 0.7 * V_{TD}}$

III. MISSION SPECIFICATION

The aircraft undergoes simple mission: start-up (1), taxi (2), take-off (3), climb to cruise altitude (4), cruise (5), loiter (6), descend (7), and land on the runway (8).

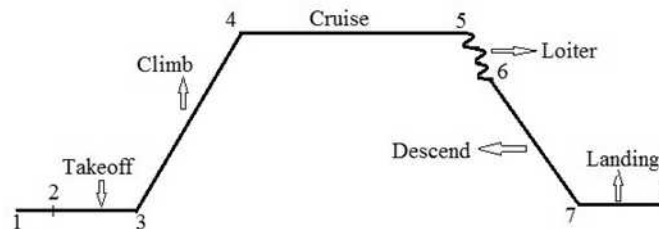


Figure 2: Mission Specification

The aircraft is expected to carry 180 passengers, 2 crew members- a pilot and a co-pilot, and 6 cabin attendants, assuming one attendant for every 30 passengers. The desired range of aircraft, which is obtained by historical data of similar category aircraft, is 5676 km, followed by an hour loiter. The aircraft will be cruising at an altitude of 11,277 m (37,000 ft) and the cruising Mach number is $M = 0.68$.



IV. WEIGHT ESTIMATION

The airplane must meet the demanding range, endurance, and cruise speed objectives while carrying its payload. It is therefore important to predict the minimum aircraft weight and fuel weight required to accomplish the given mission.

Payload weight is calculated by assuming the average weight of each passenger and baggage to be 75 kg and 25 kg respectively. The same assumptions are used to calculate the crew weight. The approximate take-off weight is determined by historical data, by comparing the weights of similar aircraft. The average fuel consumed ratio in each mission profile is then determined [reference-1]. Then mission fuel fraction weight is determined by using Equation-IV.

The fuel weight is calculated using $W_{TO(guess)}$ and M_{FF} ; Eqn-V. The approximate operational empty weight is validated by using Eqn-VI, and thereby substituting the same in Eqn-VII to get W_{TO} . Iterations are carried out by using Eqn-VIII until $W_{E(tentative)}$ and W_E become equal. Using the obtained W_{TO} , required weights are calculated.

Table 1: WEIGHT DATA	
Weight	kg
Passenger weight, W_{PL}	18,000
Crew weight, W_{crew}	800
Take-off guess weight, $W_{TO(guess)}$	65,770
Mission fuel fraction weight ratio, M_{FF}	0.731
Fuel weight, W_{fuel}	17,692.13
Approximate operational weight, $W_{OE(tentative)}$	33,210.91
Take-off weight validation, W_{TO}	83,169.39
Take-off weight after iteration, W_{TO}	67310.31
Fuel weight, W_{fuel}	18,106.47
Payload weight, W_{PL}	18,800

V. POWER-PLANT SELECTION

Again, from the historical and comparative data, the engine is selected. The aircraft will require the thrust about 220 kN. To achieve the desired thrust, two high-bypass turbofan engines are chosen, each producing a minimum thrust of 110 kN. Each engine is mounted below the wing by the help of pylons, at 6.78 m from the aircraft centerline. The type of engine which would meet the design standards will be IAE-V2527-A5.

Table 2: ENGINE DATA	
Type	IAE V-2527-A5
Thrust	118.32 kN
Bypass ratio	4.8:1
Compression ratio	32.8:1
Fan diameter	1.613 m
Length of engine	3.2 m
Weight	2,359 kg

VI. WING GEOMETRY

The geometry of the wing is mainly described by- its planform shape, its aspect ratio, the type of airfoil at wing root and tip, the thickness of wing along the span, wing sweep angle, taper ratio, and geometric twist. The taper ratio is obtained from reference-1, and it is found to be 0.24. Other geometric aspects like the wingspan, wing area, and aspect ratio are found from the analytical results of historical data, and they are found to be 34.09 m, 122.6 m², and 9.47, respectively.

From these parameters, wing root chord and wingtip chord is calculated by using Eqn-IX. Also, length of mean aerodynamic chord and its relative distance from the aircraft centerline is calculated by using Eqns-X, and XII, respectively.

The location of the wing plays a key role in the stability of the airplane. Aircraft having high-wing are comparatively more stable in lateral and rolling motion. While the aircraft with mid-wing have less interference drag and gives the best stability if the wing is dihedral. Whereas the low wing aircraft are more stable than mid-wing aircraft, but as stable as high-wing aircraft. But, low-wing configuration is mostly employed because of its structural advantage and ease of landing gear retraction into the wing box.

Table 3: WING GEOMETRIC DATA	
Root chord length	5.8 m
Tip chord length	1.392 m
Mean aerodynamic chord length	4.046 m
Distance of mean aerodynamic chord from aircraft center line	6.78 m

Selection of airfoil is the key phase in the wing geometry. The airfoil should not only reduce the form drag but also should provide enough pressure distribution around its surface to contribute in the generation of lift. The airfoil which would match the design requirements is NACA 66(4)-221. The advantage of choosing NACA 6-digit airfoil is that it maintains laminar flow over the large part of the chord and they maintain $C_{D(min)}$ compared with 4 or 5-digit airfoils.

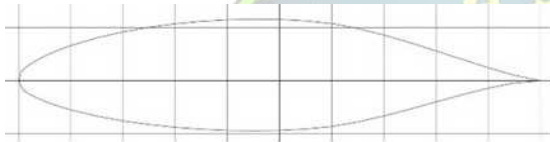


Figure 3: NACA 66(4)-221 airfoil.

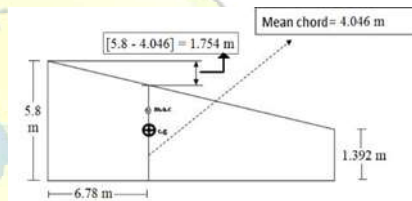


Figure 4: Wing geometry

VII. FUSELAGE SIZING

The role of the fuselage is to hold the other parts of aircraft. Its major function is to provide overall structural integrity and house for the payload. The fuselage is also expected to maintain the pressurization inside the cabin and the cockpit. The fuselage is divided into sections, such as, nose, cockpit, cabin, and tail fuselage. The cockpit is where all the controllers, navigational systems, etc., are placed. The cabin houses the payload. The major geometric parameters that decide the cabin are cabin diameter and its length. These in turn are decided by more specific details like number of seats, the width of each seat, the arrangement of seats, pitch of the seat, aisle width, and lastly, the number of aisles. The typical seating abreast is 6 with one aisle. The number of seats across will fix the number of rows in the cabin, and thereby the cabin length.

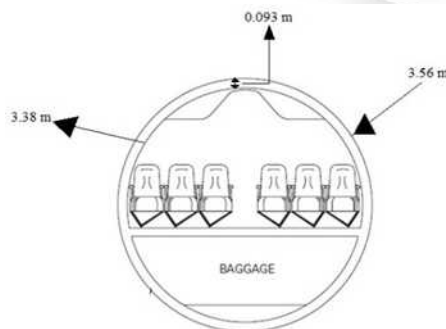


Figure 5: Fuselage cross section

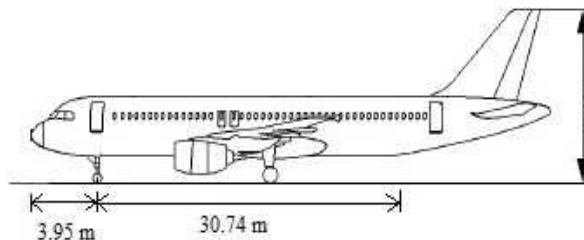


Figure 6: Fuselage sizing



The length of the fuselage is determined by using the Eqn-XII. Also, the geometric parameters of the fuselage, as stated above are calculated using the Eqn XII, XIV, XV, and XVI. The profile of the rear fuselage is chosen to provide a smooth (lesser drag) shape which also supports the horizontal stabilizers and tail. It houses the Auxiliary Power Unit (APU). The lower profile of the rear fuselage must provide adequate clearance for aircraft during take-off. The length of the tail is determined by using the Eqn-XVII.

Table 4: FUSELAGE SIZING DATA	
Length of fuselage, L_{fus}	34.18 m
Length of nose, L_{nose}	1.024 m
Length of cabin, L_{cabin}	30.74 m
Internal diameter of the fuselage, $d_{fus(internal)}$	3.38 m
External diameter of the fuselage, $d_{fus(external)}$	3.56 m
Structural thickness, $t_{structural}$	0.093 m
Length of the tail, L_{tail}	8.188 m

VIII. AERODYNAMIC CHARACTERISTICS

A. Lift

Lift is mainly due to the pressure distribution on the surface of the wing. The amount of lift depends on the planform area, air density, velocity of aircraft, and lift coefficient. This component of aerodynamic force (lift) is generated on aircraft, perpendicular to the direction of flight. The lift coefficient, C_L , is a measure of lift effectiveness and mainly depends upon section shape, the angle of attack, compressibility effects (Mach number), planform geometry, and viscous effects (Reynold's number). The role of C_L plays vital during low speeds, especially during landing and takeoff. During these maneuvers, high lift is desired, which is obtained by increasing the C_L . High lift devices are installed on the surface of the wing to achieve high C_L . They change the net angle of attack, and increase the surface area, thereby obtaining high lift.

The value of lift keeps varying along the mission phases. Lift is high during takeoff and landing, comparatively lesser during climb and descend phases, and lift is equal to the weight of the aircraft during the cruise, as the aircraft will neither gain nor lose altitude.

The lift is estimated using the Eqn-XVIII, considering the changes in flight velocity, density, and C_L , as the aircraft gains or loses altitude.

Table 5: LIFT ESTIMATION DATA		
Lift During	CL	Lift value in Kn
Takeoff	2.508	1178.94
Cruise	0.663	660.31
Landing	3.058	1383.61

B. Drag

The component of aerodynamic force which acts opposite to the direction of flight, which reduces the overall performance of the airplane, is called drag. There are many factors due to which the drag would arise. Of those factors, the main contributors are, skin friction drag- which arises due to shear stresses produced in the boundary layer, form drag- which arises due to the shape of the body, and due to the static pressure distribution around the surface of the body, and wave drag- which arises due to the presence of shockwaves on wings and fuselage, propeller blade tips moving at transonic and supersonic speeds.

The amount of drag depends on air density, planform area, aircraft's velocity, and drag coefficient. The value of drag can be estimated by using Eqn-XIX. But, the value of drag is not only dependent on above-mentioned parameters, it also depends on the alignment of aircraft with the relative head wind, cleanliness and surface roughness of aircraft skin, the maneuvering of aircraft, the effect of angle of incidence, etc. Hence, the drag value is a variable quantity, and it can only be determined if all the dependent variables are known.

IX. LANDING GEAR CONFIGURATION

The basic type of landing gear used are- tandem landing gear, tail-wheel type landing gear (conventional gear), and tricycle-type landing gear.



In tandem landing gear, the main gear and tail gear are aligned to the longitudinal axis of the airplane. The aircraft which use this type of landing gear is military bombers B-47 and the B-52, and few gliders are configured with tandem landing gear. In tail wheel-type landing gear arrangement, the main gear is located forward of the c.g, causing the tail to require support from the third wheel assembly. Maule MX-235 Super Rocket and McDonnell Douglas DC-3 use this type of landing gear arrangement. The landing gear configuration which finds more application in civil aircraft is tricycle-type landing gear. The advantage of using this type of arrangement in civil aircraft is that it prevents ground-looping of the aircraft, and it allows more forceful application of the brakes without noising over when braking, which is advantageous during higher landing speeds.

The landing gear arrangement which meets the design standards is tri-cycle type arrangement, with 4 wheels in the main landing gear (two on each axle) and 2 on the nose landing gear.

The geometry of the wheels is calculated by using Eqn-20, by substituting the values of A and B as given in Table-6. The weight acting on each main landing wheel is 18,426 kg and that on nose landing wheel is 16,152 kg.

Table 6: LANDING GEAR SIZING DATA		
	A	B
Wheel diameter	1.63 inch	0.315 inch
Wheel width	0.1043 inch	0.48 inch

To determine the position of landing gear, aerodynamic and geometric parameters of the wing is considered. The static margin is assumed to be 18% and the position of the neutral point (X_{NP}) is determined using Eqn-XXI. The horizontal tail volume ratio and lift slope ratio of tail to wing is taken from the historical and analytical data, and it is found to be 0.253 and 4.545, respectively. The location of the main landing gear is at the center of the wing.

Table 7: LANDING GEAR WHEEL DATA		
	Main landing gear	Nose landing gear
Wheel diameter	0.91 m	0.876 m
Wheel width	0.29 m	0.277 m

Table 8: LANDING GEAR POSITION DATA	
Position of neutral point from aircraft nose, X_{NP}	19.14 m
Position of aerodynamic center of wing, $X_{(ac)wing}$	17.98 m
Position of main landing gear from aircraft nose	19.27 m
Position of nose landing gear from aircraft nose	3.95 m

X. RANGE AND ENDURANCE

A. Range

The range is the total distance covered by the aircraft during its mission on one load fuel. The range of an aircraft depends on the weight of fuel it is carrying, the engine's thrust specific fuel consumption (TSFC), cruising altitude, wing planform area, and $\frac{C_L^{1/2}}{C_D}$ -ratio. The flight conditions for maximum range for a jet-propelled airplane are- the aircraft should fly at a high altitude where the free stream air density is small; the engine should have lowest possible TSFC; the aircraft should carry a lot of fuel, and the aircraft should fly with a maximum $\frac{C_L^{1/2}}{C_D}$. The range is calculated using the Eqn-II, and it is found to be 6025.10 km.

B. Endurance

Endurance is the total time that an airplane can stay in the air on one load of fuel. The range of an aircraft depends on the weight of fuel, the engine's TSFC, and L/D ratio. For an aircraft to have maximum endurance, it should carry a lot of fuel; the engine should have lowest possible TSFC, and the aircraft should fly at maximum (L/D). The range is calculated by using the Eqn-II, and it is found to be 16.7 hours. But, practically, the aircraft will not have such endurance. The aircraft belonging to the design requirement category



possess endurance of 5 to 7 hours. Since the calculation is done considering the maximum dependent parameters, such a huge value of endurance is achieved.

XI. TAKEOFF PERFORMANCE

The takeoff distance for an airplane is the total distance covered by the airplane, with respect to the ground, from the point of release of brakes (mission point-2) to the point where the airplane cleared the obstacle height. The takeoff distance is primarily divided into two phases- ground roll distance, and distance while airborne to clear an obstacle. The obstacle height for the military airplane is 50 feet, and for civil aircraft is 35 feet.

The ground roll distance is the total distance covered by the aircraft from the point of release of brakes to the point where the aircraft becomes airborne. During takeoff, the airplane would require a greater lift, which is obtained by increasing the coefficient of lift with the help of high lift devices. The ground roll is calculated by using the Eqn-XXIII. During this phase, the flaps are extended and kept at takeoff position of 20° , so that the maximum coefficient of lift will be increased to 2.508.

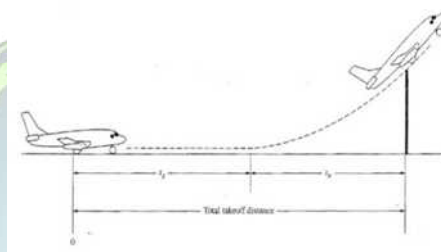


Figure 7: Illustration of ground roll (s_g), and airborne distance (s_a)

The flight path after liftoff is essentially pull-up maneuver in the radius 'r'. The turn radius is calculated using the Eqn-XXIV. The angle induced by the flight path between the point of takeoff and that for clearing the obstacle height is θ_{OB} . During this phase, the airplane will cover a distance, S_a , which is calculated by using the Eqn-XXV.

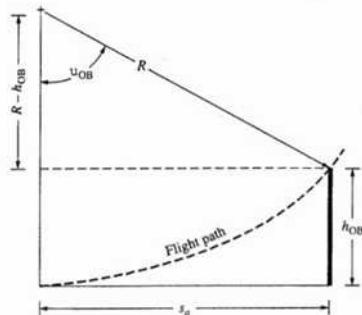


Figure 8: Illustration of obstacle airborne distance.

Table 9: TAKEOFF DISTANCE DATA	
Elevation	6.7 m
Density	1.225 kg/m ³
Ground roll distance	603.35 m
Airborne distance	336.27 m
Total takeoff distance	939.62 m

XII. LANDING PERFORMANCE

The landing distance begins when the airplane clears an obstacle. The landing distance is majorly classified into three phases- approach distance, flare distance, and ground roll. The distance measured along the ground from obstacle to the point of initiation of flare is called approach distance. It can be calculated by using the Eqn-XXVIII. The airplane then begins to flare, which is the transition from the straight approach path to the horizontal ground roll. The transition path is a pull-up maneuver in the turn radius ' r_{flare} ', which can be calculated from the Eqn-XXVI. The flare is initiated from a height ' h_f ', measured from the ground, and it can be calculated by using the Eqn-XXVII. The angle induced by the flight path between the point of initiation of flare



to the point of touchdown is called flare angle, Θ_f . The flare angle will be almost equal to the approach angle, which is about 3° . The flare distance can be calculated by using the XXIX.

After the point of touchdown, the aircraft will freely roll down the runway for about 3 seconds, then the pilot applies thrust reversers, releases the spoilers, and other braking systems to bring the aircraft to halt. The distance covered by the airplane from the point of touchdown to the point its velocity becomes zero is called the ground roll. It can be calculated by using the Eqn-XXX.

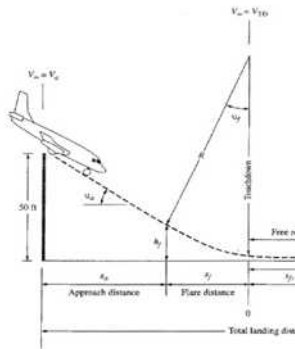


Table 10: LANDING DISTANCE DATA	
Elevation	6.7 m
Density	1.225 kg/m ³
Approach distance	112 m
Flare distance	358 m
Ground roll distance	458.29 m
Total landing distance	928.29 m

Figure 8: Illustration of landing distance.

The flare velocity is typically taken as 1.23 times the stall velocity, and the touchdown velocity (V_{TD}) is assumed as 1.15 times the stall velocity.

CONCLUSION

The aircraft design methodology is presented in this paper. The methodology gives a brief design framework in which weight estimation; selection of power-plant; design criteria for wings, fuselage, and landing gear; and performance evaluation is studied in a coherent fashion. The design and calculation of 180-seater passenger aircraft have been illustrated, and the skin-model is created by using CATIA-V5R20. The obtained results are closely associated with the actual data of the aircraft of the twin-turboprop medium-range category.

DESIGN POINTS

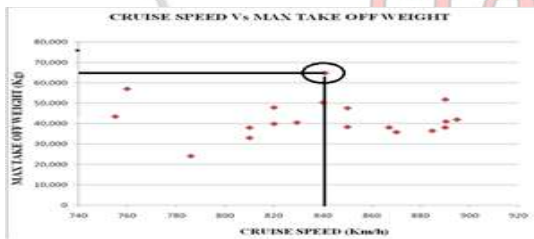


Figure 13: Cruise speed vs takeoff weight

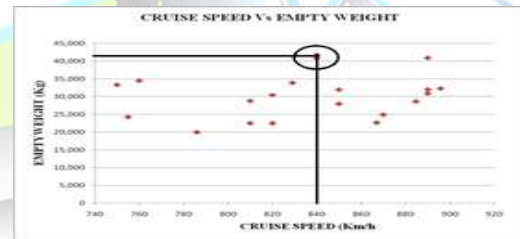


Figure 14: Cruise speed vs Empty weight

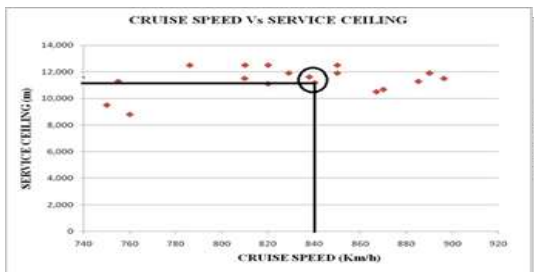


Figure 15: Cruise speed vs service ceiling

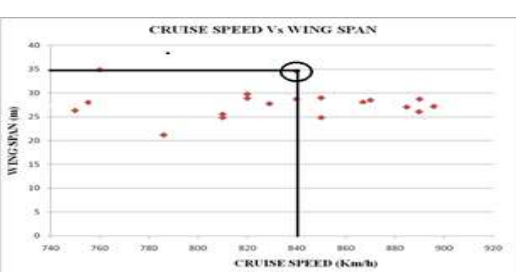


Figure 16: Cruise speed vs wing span

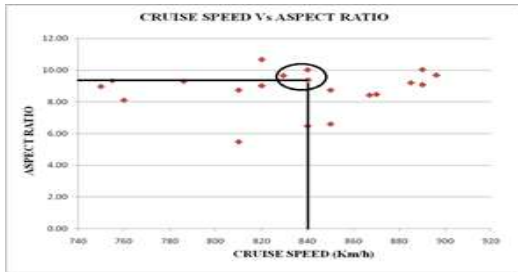


Figure 17: Cruise speed vs aspect ratio

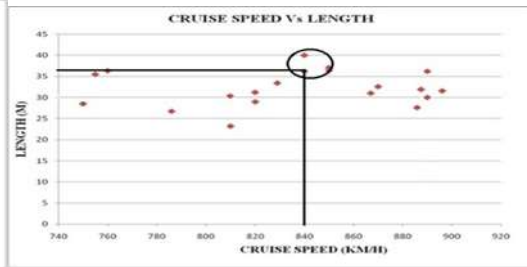


Figure 18: Cruise speed vs length of aircraft

REFERENCES

- [1] Dr. Jan Roskam, "Airplane Design", 3rd edition, Roskam Aviation and Engineering Cooperation, Kansas, 1989.
- [2] John D Anderson, "Introduction to Flight", 2nd edition, McGraw-Hill.
- [3] Daniel P Raymer, "Aircraft Design: A Conceptual Approach", 4th edition, AIAA Education Series, American Institute of Aeronautics and Astronautics, Inc., Washington, DC, 1982.
- [4] Christo Ananth, "A Novel NN Output Feedback Control Law For Quad Rotor UAV", International Journal of Advanced Research in Innovative Discoveries in Engineering and Applications [IJARIDEA], Volume 2, Issue 1, February 2017, pp:18-26.
- [5] Mohammed Sadraey, "Wing Design", Section 5.4.6, Daniel Webster College.
- [6] Lloyd R Jenkinson and James F Marchman III, "Aircraft Design Projects", 2003.
- [7] "Theory of Wing Section", report NACA-824, NASA TN-D-7428.
- [8] Egbert Torenbeek, "Advanced Aircraft Design, Conceptual Design, Technology and Optimization of Subsonic Civil Airplanes", 1988.
- [9] A P Hetteema, 'Vertical Tail Design', Delft University of Technology.
- [10] Perkins C and Hage R, "Aircraft Performance Stability and Control", Wiley, New York, 1963.
- [11] Nelson R C, "Flight Stability and Automatic Control", McGraw-Hill, 1998.

